Industrial Crops and Products 84 (2016) 230–240

Contents lists available at ScienceDirect

Industrial Crops and Products

journal homepage: www.elsevier.com/locate/indcrop

Modeling and analysis of the creep behavior of jute/green epoxy composites incorporated with chemically treated pulverized nano/micro jute fibers

Abdul Jabbar[a], Jiří Militký[a,*], Bandu Madhukar Kale[a], Samson Rwawiire[a], Yasir Nawab[b], Vijay Baheti[a]

[a] Department of Material Engineering, Technical University of Liberec, Studentská 2, 461 17 Liberec, Czech Republic
[b] Department of Fabric Manufacturing, National Textile University, Faisalabad 37610 Pakistan

ARTICLE INFO

Article history:
Received 7 November 2015
Received in revised form 7 December 2015
Accepted 19 December 2015

Keywords:
Jute fiber
Polymer composites
Creep
Green epoxy
Compression molding
Pulverization

ABSTRACT

This paper reports the creep behavior of alkali treated jute/green epoxy composites incorporated with various loadings (1, 5 and 10 wt%) of chemically treated pulverized jute fibers (PJF) at different environment temperatures. Composites were prepared by hand layup method and compression molding technique. The creep and dynamic mechanical tests were performed in three-point bending mode by dynamic mechanical analyzer (DMA). The incorporation of PJF is found to significantly improve the creep resistance and strain rate of composites. Three creep models i.e. Burger's model, Findley's power law model and a simpler two-parameter power law model were used to model the creep behavior in this study. The time temperature superposition principle (TTSP) was applied to predict the long-term creep performance. The Findley's power law model was found to be satisfactory in predicting the long-term creep behavior. Dynamic mechanical thermal analysis (DMTA) results revealed the increase in storage modulus, glass transition temperature and reduction in the tangent delta peak height of composites with higher loading of PJF.

© 2015 Elsevier B.V. All rights reserved.

1. Introduction

Natural fiber polymer composites (NFPC) are increasingly used nowadays in industrial applications as a substitute of polymer composites made with mostly used synthetic fibers such as glass and carbon etc. due to their environmental and economic benefits. Natural fibers are renewable, biodegradable, cost effective, safe to use, available in huge quantities, low fossil-fuel energy requirements and the most importantly their high specific strength to weight ratio (John and Anandjiwala, 2009; Mishra et al., 2003). This is of distinctive importance especially in interior transportation applications as it leads to reduction of vehicle weight for higher fuel efficiency and energy saving. Polymer composites used in engineering applications are often subjected to stress for a long time and at high temperatures. Creep (a progressive deformation of a material at constant stress) is very important end-use property for material applications requiring long term durability and reliability (Krempl and Khan, 2003). Considerable studies can be found in literature on the creep behavior of natural fiber polymer composites. Different mathematical modeling techniques have also been applied to analyze the creep behavior of composite materials (Acha et al., 2007; Bledzki and Faruk, 2004; Hao et al., 2014; Jia et al., 2011; Marcovich and Villar, 2003; Xu et al., 2010). Researchers have also tried to study the creep behavior of polymer composites by addition of different kinds of fillers in matrices (Jia et al., 2011; Shen et al., 2004; Siengchin, 2013; Siengchin and Karger-Kocsis, 2009; Yang et al., 2006a,b). Addition of nano/micro fillers to polymers has shown improvements in the strength and stiffness of the resulting composites, however, research shows that these fillers tend to plasticize the composites. To the author's best knowledge, there is no study available in open literature on the creep behavior of alkali treated jute reinforced green epoxy composites incorporated with chemically treated pulverized jute fibers as reinforcing fillers. Among all the natural reinforcing materials, jute appears to be a promising fiber due to its high toughness and aspect ratio in comparison with other natural reinforcements (Acha et al., 2007) and occupies the second place in terms of world production levels of cellulosic fibers (Cai et al., 2000). The objective of the present study is to investigate the incorporation of pulverized nano/micro jute fibers prepared from waste jute on the creep behavior under

* Corresponding author.
E-mail address: jiri.militky@tul.cz (J. Militký).

http://dx.doi.org/10.1016/j.indcrop.2015.12.052
0926-6690/© 2015 Elsevier B.V. All rights reserved.

the conditions of different temperatures and dynamic mechanical behavior of alkali treated woven jute/green epoxy composites. The modeling of experimental creep data is satisfactorily conducted using different creep models. Furthermore, the time-temperature superposition principle (TTSP) is employed in order to predict the long-term creep behavior of composites based on experimental data.

2. Materials and methods

2.1. Materials

Jute woven fabric produced from tossa jute (*Corchorus olitorius*) fibers having an areal density of 600 gm^{-2} with 5-end satin weave design was produced on a shuttle loom. Warp and weft densities of the fabric were 6.3 threads per cm and 7.9 threads per cm respectively. Waste jute fibers, sourced from a jute mill, were used for pulverization. Green epoxy resin CHS-Epoxy G520 and hardener TELALIT 0600 were supplied by Spolchemie, Czech Republic. Sodium hydroxide (NaOH) was supplied by Lach-Ner, Czech Republic. Sodium sulfate (Na_2SO_4) and sodium hypochlorite (NaOCl) were supplied by Sigma–Aldrich, Czech Republic.

2.2. Chemical pretreatment

The untreated fabric was first washed with 2 wt% non-ionic detergent solution at 70 °C for 1.0 h prior to surface treatments to remove any dirt and impurities sticking to the surface. The jute fabric and waste jute fibers were then immersed separately in 2% NaOH solution for 1 h at 80 °C maintaining a liquor ratio of 15:1. Alkali treated waste jute fibers were further treated with 7 g/l NaOCl solution at room temperature for 2 h under pH 10–11 and subsequently antichlored with 0.1% Na_2SO_4 at 50 °C for 20 min. Both fabric and waste fibers, after chemical pretreatment, were then washed with fresh water several times until the final pH was maintained at 7.0 and then allowed to dry at room temperature for 48 h and at 100 °C in an oven for 2 h.

2.3. Pulverization of jute fibers

Pulverization of chemically treated waste jute fibers was carried out using a high-energy planetary ball mill of Fritsch pulverisette 7. Pulverization process relies on the principle of energy release at the point of impact between balls as well as on the high grinding action created by friction of balls on the wall (Baheti and Militky, 2013). The sintered corundum container of 80 ml capacity and zirconium balls of 10 mm diameter were chosen for 1 h of pulverization. The ball to material ratio (BMR) was kept at 10:1 and the speed was kept at 850 rpm.

2.4. Preparation of composites

The composites were prepared by hand layup method. The resin and hardener were mixed in a ratio of 100:32 (by weight) according to manufacturer recommendations and then weighed amounts of pulverized jute fibers (PJF) under 1, 5 and 10 wt% were mechanically mixed with epoxy resin at room temperature until a homogeneous mixture was obtained. The prepared resin/PJF mixture was poured on fabric layers and spread out by a hand roller. The gentle rolling action of hand roller confirmed the wetting of jute fabrics. Each composite laminate comprised 3 layers of jute fabric with orientation of each layer in the same direction. The composite layup along with Teflon sheets were sandwiched between a pair of steel plates and cured at 120 °C for 1.0 h in a mechanical convection oven with predetermined weight on it to maintain uniform pressure of about 50 kPa (Mishra et al., 2014). The fiber volume fraction (V_f) of all composites was in the range of 0.25–0.27. The prepared composite samples were designated as U (untreated), A-0% (alkali treated jute fabric with 0 wt% of PJF), 1%, 5% and 10% (alkali treated jute fabric with 1, 5, 10 wt% of PJF) respectively.

2.5. Characterization and testing

2.5.1. Characterization of pulverized jute fibers

The untreated and treated jute fabric and fibers were analyzed by FTIR spectroscopy. A Thermo Fisher FTIR spectrometer, model Nicolet iN10, was used in this study. The spectrometer was used in the absorption mode with a resolution of 4 cm^{-1}. Particle size distribution of pulverized jute particles was studied on Malvern Zetasizer nano series based on dynamic light scattering principle of Brownian motion of particles. Deionized water was used as dispersion medium and it was ultrasonicated for 5 min with BANDELIN ultrasonic probe SONOPLUS before characterization. Refractive index of 1.52 was used to calculate particle size of pulverized jute. In addition, morphologies of pulverized jute fibers were observed with Vega-Tescan TS5130 Scanning Electron Microscope at 30 KV accelerating voltage. The surface of fibers was gold coated prior to SEM inspection.

2.5.2. Characterization of composites

Short-term creep tests were performed in three point bending mode at temperatures 40 °C, 70 °C and 100 °C using Q800 Dynamic mechanical thermal analysis (DMTA) instrument of TA instruments (New Castle DL, USA) for 30 min. The static stress of 2.0 MPa was applied at the center point of long side of the sample through the sample thickness for 30 min after equilibrating at the desired temperature and creep strain was measured as a function of time. The static stress was selected after performing a strain sweep test, where the linear viscoelastic region was defined for each of the composites ensuring that the creep tests were conducted in the linear viscoelastic region. The TTSP was selected for short-term creep tests performed at various temperatures for jute/green epoxy composites incorporated with various contents of PJF. The temperature range was 40–100 °C, in 5 °C steps, and the isothermal tests were run on the same specimen in the temperature range. The 2.0 MPa stress was applied for 10 min at each temperature. In every measurement, the specimen was equilibrated for 5 min at each temperature, in order to evenly adjust for the correct temperature of the specimen. The dynamic mechanical properties of composites were measured in 3-point bending mode using the above same instrument. The testing conditions were controlled in the temperature range of 35–200 °C, with a heating rate of 3 °C/min, fixed frequency of 1 Hz, preload of 0.1 N, amplitude of 20 μm, and force track of 125%. The samples having a thickness of 4.5–5 mm, width of 12 mm and span length of 50 mm were used for both creep and DMTA testing. Two replicate samples were tested for each test condition and average values are reported.

2.6. Creep modeling

The non-linear curve fit function of the OriginPro 9.0 software was used for modeling the creep curves and fitting the models to the experimental data. The minimum sum of squared deviation of experimental data from the creep models and correlation coefficient (R^2) were selected as criterion (Meloun and Militky, 2011). The correlation coefficient value R^2 is defined as model sum of squares divided by total sum of squares. A better goodness-to-fit is obtained when R^2 is closer to 1.

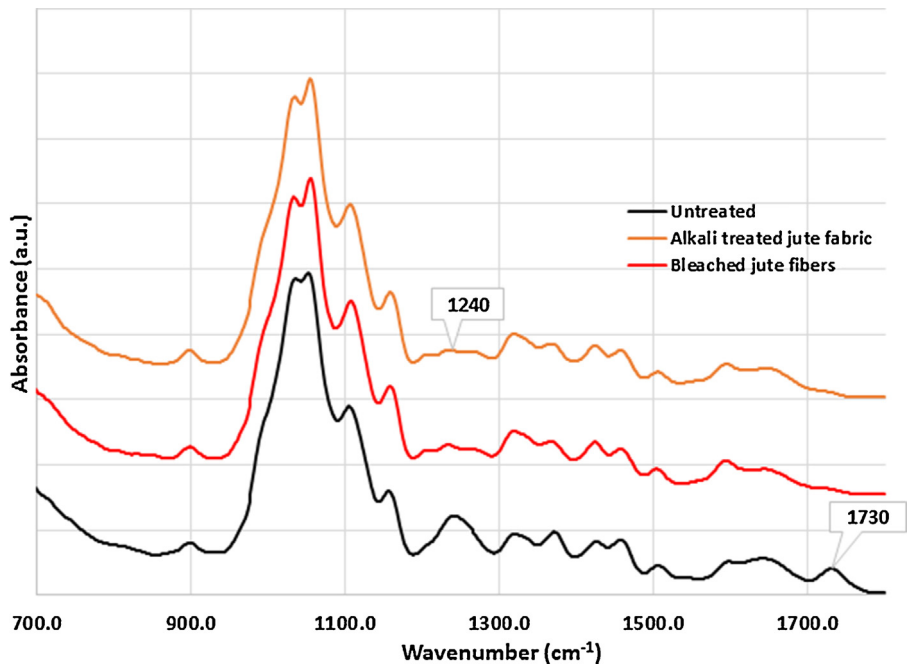

Fig. 1. FTIR spectra of jute fibers.

3. Results and discussion

3.1. Characterization of jute fibers

FTIR analysis was carried out to confirm some removal of non-cellulosic contents (e.g. hemicelluloses and lignin) from the surface of jute fibers after pretreatments. The FTIR spectra of untreated and treated jute are shown in Fig. 1. The major difference observed between the spectra is the disappearance/reduction of peaks at ~1730 cm^{-1} and ~1240 cm^{-1}. The peak at ~1730 cm^{-1} is due to stretch vibration of C=O bonds in carboxylic acid and ester components of cellulose and hemicellulose (Morshed et al., 2010) and also a chemical group of lignin (Haque et al., 2009; Tserki et al., 2005). The peak at ~1240 cm^{-1} is due to C—O—C asymmetric stretching of the acetyl group of lignin (Liu et al., 2004). The reduction/disappearance of these peaks confirm the partial removal of hemicellulose and opening up of the lignin structure in the jute fibers after pretreatments.

The jute fibers were pulverized to particles with an average size of 1480 nm in wider particle size distribution as shown in Fig. 2a. Fig. 2b shows the shape and surface morphology of pulverized jute fibers. The PJF can be seen in irregular shape and size with certain aspect ratio as well.

3.2. Creep behavior

3.2.1. Creep models

Four parameters (or the Burger's) model is one of the mostly used physical models to give the relationship between the morphology of polymer composites and their creep behavior (Findley et al., 1989; Ward and Sweeney, 2012). It is based on a series combination of a Maxwell element with a Kelvin–Voigt element. The total creep strain is divided into three separate parts: ε_M the instantaneous elastic deformation (Maxwell spring), ε_K viscoelastic deformation (Kelvin unit) and ε_∞ viscous deformation (Maxwell dash-pot). Thus, total strain as a function of time can be represented by the following equations:

$$\varepsilon(t) = \varepsilon_M + \varepsilon_K + \varepsilon_\infty \quad (1)$$

$$\varepsilon(t) = \frac{\sigma_0}{E_M} + \frac{\sigma_0}{E_K}\left(1 - e^{-E_K t/\eta_K}\right) + \frac{\sigma_0}{\eta_M} t \quad (2)$$

Where $\varepsilon(t)$ is the creep strain, σ_0 is the stress, t is the time, E_M and E_K are the elastic moduli of Maxwell and Kelvin springs, and η_M and η_K are the viscosities of Maxwell and Kelvin dashpots. η_K/E_K is usually denoted as τ, the retardation time required to generate 63.2% deformation in the Kelvin unit (Yang et al., 2006b). ε_M is a constant value and does not change with time. ε_K represents the earliest stage of creep and attains a saturation value in short time and ε_∞ represents the trend in the creep strain at sufficiently long time, and appears similar to the deformation of a viscous liquid obeying Newton's law of viscosity. The four parameters E_M, E_K, η_M, η_K can be obtained by fitting the Eq. (2) to the experimental data and can be used to describe the creep behavior of composites. The creep rate of viscoelastic materials can be obtained by taking the derivative of Eq. (2).

$$\frac{d\varepsilon(t)}{dt} = \frac{\sigma_0}{E_K}\left(e^{-E_K t/\eta_K}\right) + \frac{\sigma_0}{\eta_M} \quad (3)$$

The Findley's power law model is an empirical mathematical model used to simulate the creep behavior of polymer composites. The model can be represented by the following Eq. (4) (Findley et al., 1989);

$$\varepsilon(t) = at^b + \varepsilon_0 \quad (4)$$

Where, a and b are the material constants and ε_0 is the instantaneous strain. The ability of Findley's power law model to simulate the creep data has been found to be satisfactory in several studies (Jia et al., 2011; Plaseied and Fatemi, 2008; Yang et al., 2006b). However, this model is not able to explain the creep mechanism of material. A two parameter empirical power law model has also been used in some studies (Tajvidi et al., 2005; Xu et al., 2010) to simulate the creep date. It has the form;

$$\varepsilon(t) = at^b \quad (5)$$

Where, a and b are the material constants and ε_0 is the instantaneous strain.

The long term creep is an important parameter to evaluate the end-use performance of natural fiber polymer composites but it

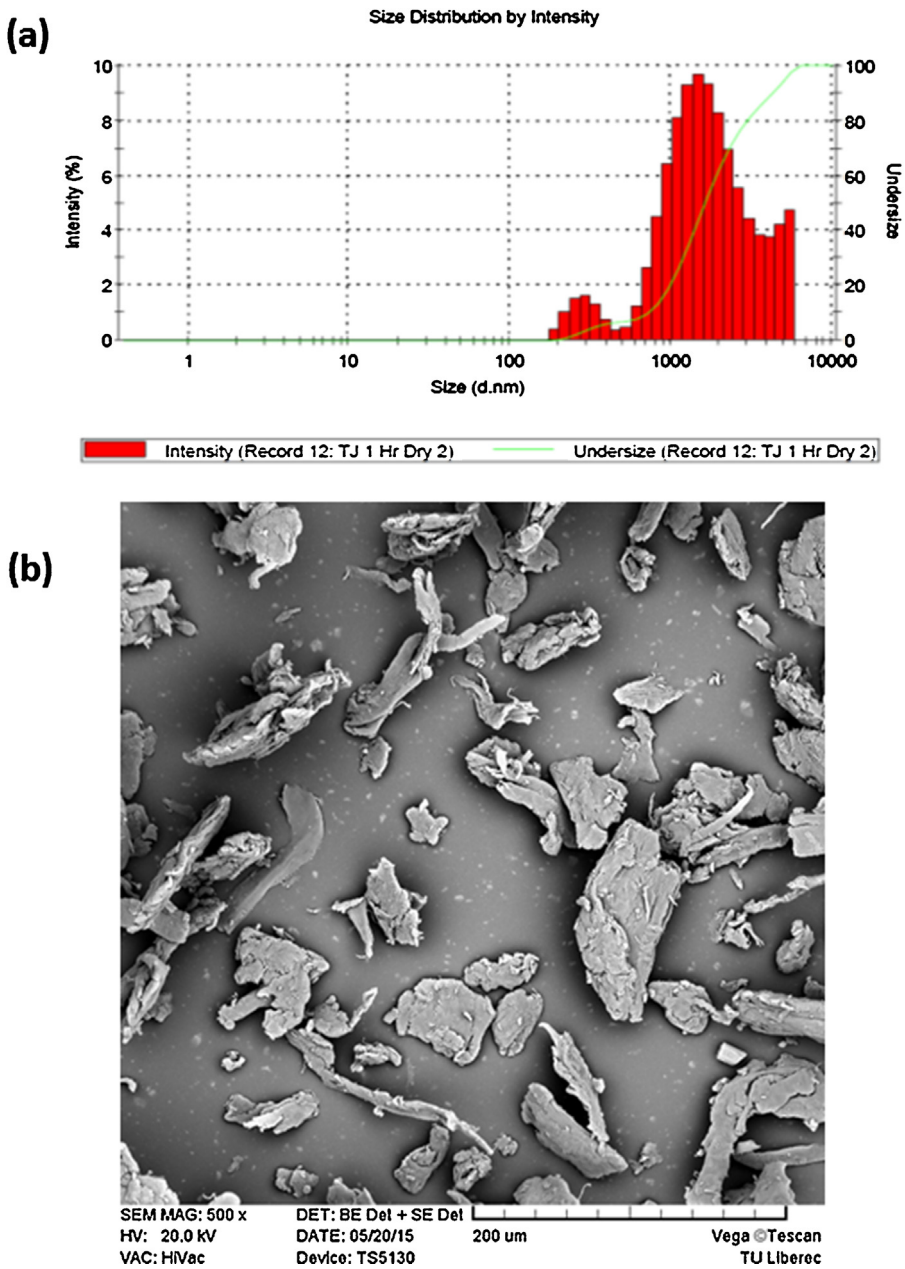

Fig. 2. (a) Particle size distribution and (b) SEM image of jute fibers after pulverization.

is often impractical to perform a creep test for an extremely long period of time. Time-temperature superposition (TTS) is one of the common estimation techniques to predict the long term creep behavior by shifting the curves from tests at different temperatures horizontally along the logarithmic time axis to generate a single curve known as master curve (Ward and Sweeney, 2012). The shifting distance is called shift factor.

3.2.2. Short term creep

Fig. 3 shows the creep strains for jute composites as a function of time with 0, 1, 5, 10 wt% of PJF content at three different temperature conditions. It is visibly apparent that the composites have low instantaneous deformation ε_M and creep strain at 40 °C due to higher stiffness of composites but this deformation increases at higher temperatures due to decrease in composites stiffness. The creep strain of all composites also increased at higher temperatures but the untreated jute composites was affected more than the others. The creep strain of alkali treated with 0% PJF composite is less than untreated one. This may be explained due to increase in surface roughness of jute fabric after alkali treatment and decrease in frictional slippage of matrix polymer chains at the fiber/matrix interface resulting in less creep deformation than untreated composite. The least creep strain is shown by composite incorporated with 10% PJF at all temperatures followed by 5% and 1% PJF incorporated composites. At 100 °C, 5% and 10% PJF composites have almost same instantaneous elastic deformation but 10% composite has less viscous deformation over time. This may be attributed to greater inhibition of slippage and reorientation of polymer chain with increasing contents of PJF. The Burger's model curves show a satisfactory agreement with the experimental data (Fig. 3). The four parameters E_M, E_K, η_M, η_K of Burger's model, used to fit the Eq. (2) to the experimental data, are summarized in Table 1. All four parameters were found to decrease for all composites as temperature increased (Table 1). E_M corresponds

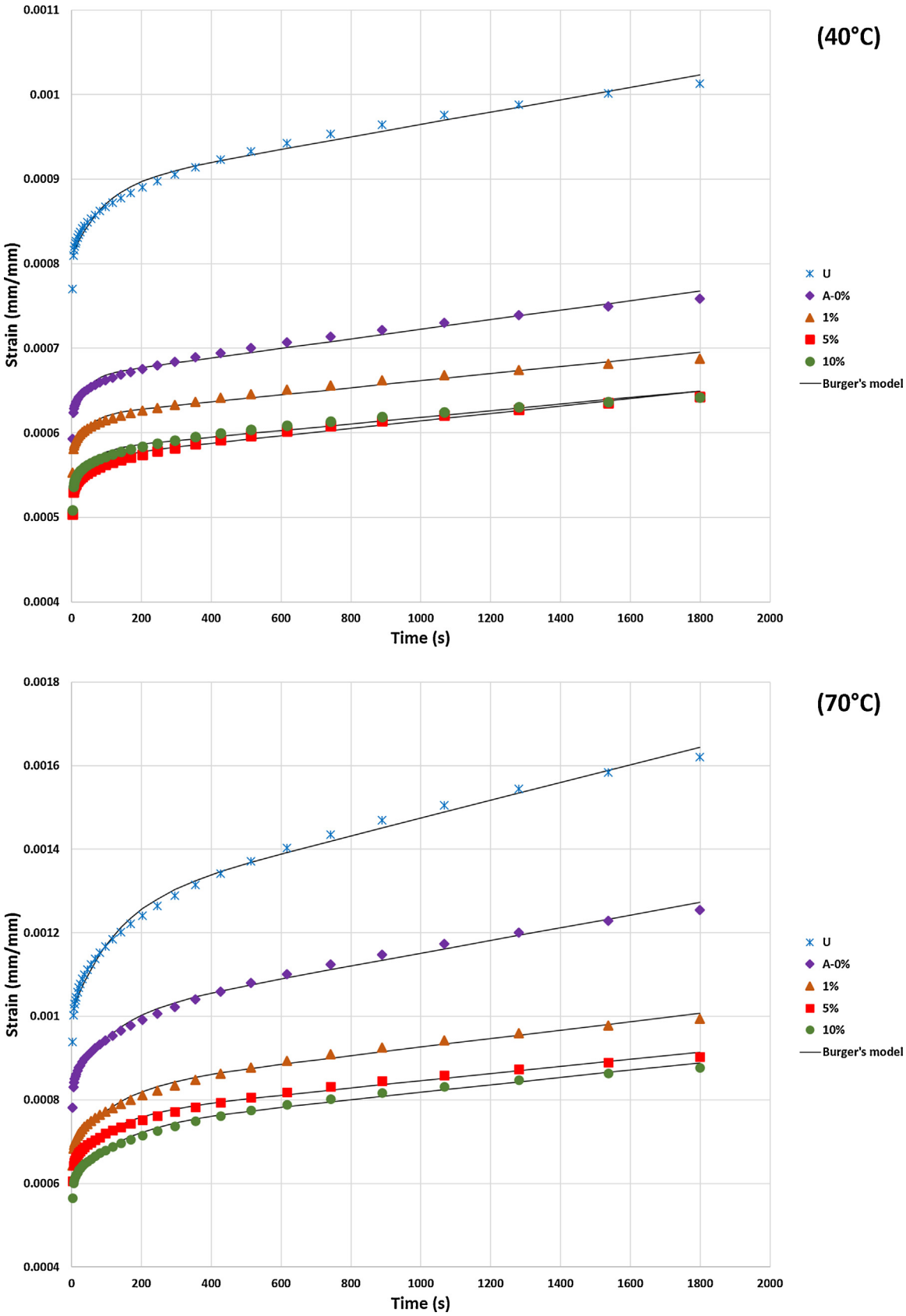

Fig. 3. Creep curves of composites incorporated with different loadings of PJF at different temperatures.

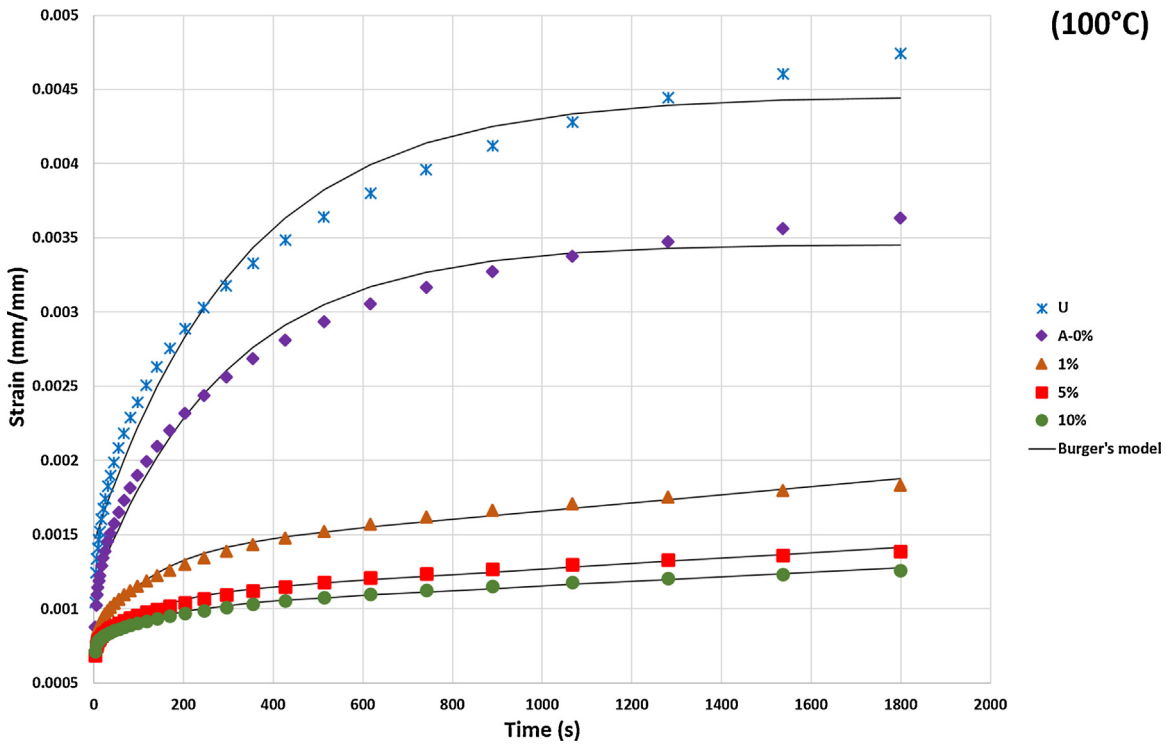

Fig. 3. *Continued.*

Table 1
Simulated four parameters in Burger's model for short term creep of the composites.

Temperature	Parameters	Composite types				
		Untreated	Alkali-0%	1%	5%	10%
40 °C	E_M (MPa)	2477.24 ± 78.3	3259.41 ± 138.0	3492.53 ± 133.8	3810.53 ± 133.6	3774.75 ± 149.1
	E_K (MPa)	23876.27 ± 10854.5	38244.62 ± 19726.9	42496.38 ± 21110.6	44220.12 ± 21281.1	40549.80 ± 19016.6
	η_M (Pa s)	2.72E7 ± 1.33E7	3.54E7 ± 1.22E7	4.77E7 ± 2.04E7	4.54E7 ± 1.97E7	5.11E7 ± 2.47E7
	η_K (Pa s)	2.11E6 ± 2.38E6	1.37E6 ± 2.09E6	1.73E6 ± 2.5E6	2.53E6 ± 3.49E6	1.90E6 ± 2.62E6
	SS*	2.65033E-9	1.29037E-9	1.04302E-9	9.92292E-10	1.08146E-9
	Adj. R^2	0.97524	0.97061	0.96424	0.96929	0.96304
70 °C	E_M (MPa)	1985.89 ± 91.9	2403.61 ± 102.7	2921.19 ± 118.5	3116.67 ± 118.6	3323.10 ± 131.9
	E_K (MPa)	7790.84 ± 2752.5	11972.90 ± 4497.3	14228.47 ± 5360.3	16946.57 ± 6037.4	15615.45 ± 5726.5
	η_M (Pa s)	9.48E6 ± 3.81E6	1.32E7 ± 5.14E6	1.98E7 ± 9.71E6	2.33E7 ± 1.08E7	2.27E7 ± 1.13E7
	η_K (Pa s)	956179.43 ± 6.90E5	1.32E6 ± 1.09E6	1.71E6 ± 1.34E6	1.81E6 ± 1.45E6	1.94E6 ± 1.44E6
	SS*	1.08937E-8	5.93037E-9	3.81543E-9	2.74811E-9	2.87718E-9
	Adj. R^2	0.98881	0.98689	0.9851	0.9847	0.98596
100 °C	E_M (MPa)	1380.05 ± 294.3	1743.43 ± 306.1	2417.83 ± 218.3	2653.56 ± 183.6	2616.45 ± 123.7
	E_K (MPa)	665.35 ± 117.7	865.63 ± 121.6	3543.54 ± 958.0	6087.72 ± 1783.7	8457.41 ± 2683.5
	η_M (Pa s)	−4.13E20 ± 0.0	−6.00E32 ± 0.0	7.44E6 ± 3.92E6	1.08E7 ± 5.26E6	1.31E7 ± 5.97E6
	η_K (Pa s)	219089.75 ± 1.03E5	255733.51 ± 9.91E4	457813.67 ± 2.43E5	705184.01 ± 4.39E5	1.11E6 ± 6.84E5
	SS*	8.30033E-7	3.37586E-7	2.87859E-8	1.31777E-8	6.79893E-9
	Adj. R^2	0.97565	0.98358	0.99023	0.98826	0.98971

SS*: Sum of squared deviations.

to the elasticity of the crystallized zones in a semicrystallized polymer. Compared to the amorphous regions, the crystallized zones are subjected to immediate stress due to their higher stiffness. The instantaneous elastic modulus is recovered immediately once the stress is removed. E_K is also coupled with the stiffness of material. The decrease in parameters E_M, E_K resulted from the increase in the instantaneous and the viscoelastic deformations as temperature increased. The viscosity η_M corresponds to damage in the crystallized zones and irreversible deformation in the amorphous regions and the viscosity η_K is associated with the viscosity of the amorphous regions in the semicrystallized polymer (Militký and Jabbar, 2015). The decrease in viscosity parameters η_M, η_K propose an improvement in the mobility of molecular chains at higher temperature. The parameters for untreated and alkali treated with 0% PJF composites have undergone a largest decrease, resulting in higher creep strain. The composites incorporated with PJF, especially 5 and 10%, have comparatively better values of parameters particularly η_M which is related to the long term creep strain and validates less temperature dependence of these composites (Fig. 3). The viscosity η_M increases with the increase in PJF% and permanent deformation decreases. Fig. 4a and b compares the creep strain and strain rate of untreated and 10% PJF composites at various temperatures. Comparatively, temperature had more influence on the creep deformation of untreated jute composite than that of 10% PJF composite.

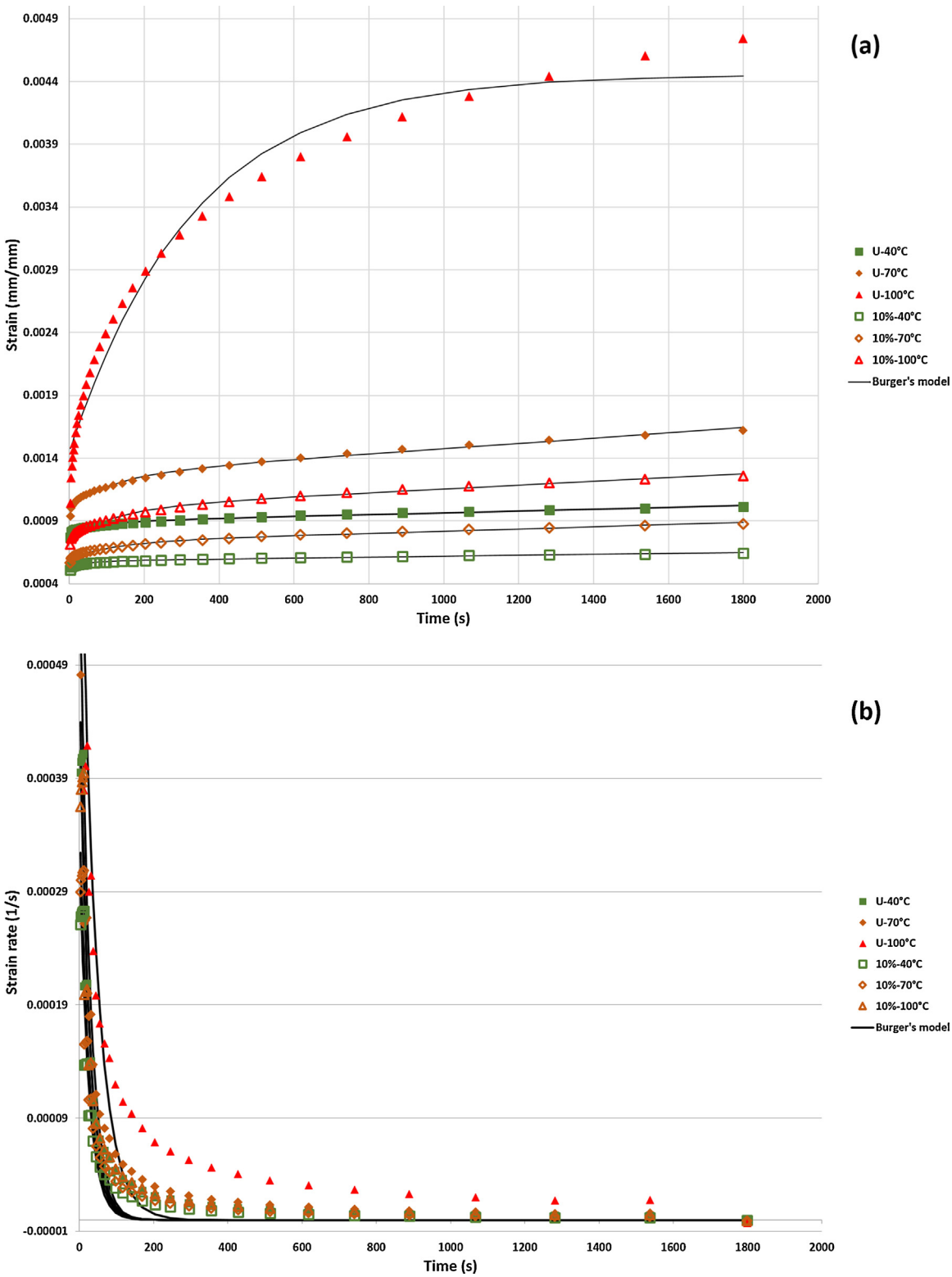

Fig. 4. Creep strain (a) and strain rate (b) of untreated and 10% PJF composites at different temperatures.

3.2.3. *Time-temperature superposition (TTS)*

The creep curves corresponding to different temperature levels were shifted along the logarithmic time axis according to time–temperature superposition principle using TA Instruments Thermal Advantage™ software to generate a master curve at a reference temperature of 40 °C. The shifting procedure of this curve obeys the Williams–Landel–Ferry (WLF) equation. The WLF equation is given by Eq. (6);

$$\log \alpha_T = \frac{-C_1 (T - T_0)}{C_2 + (T - T_0)} \tag{6}$$

Where α_T is the horizontal (or time) shift factor, C_1 and C_2 are constants, T_0 is the reference temperature (K) and T is the test

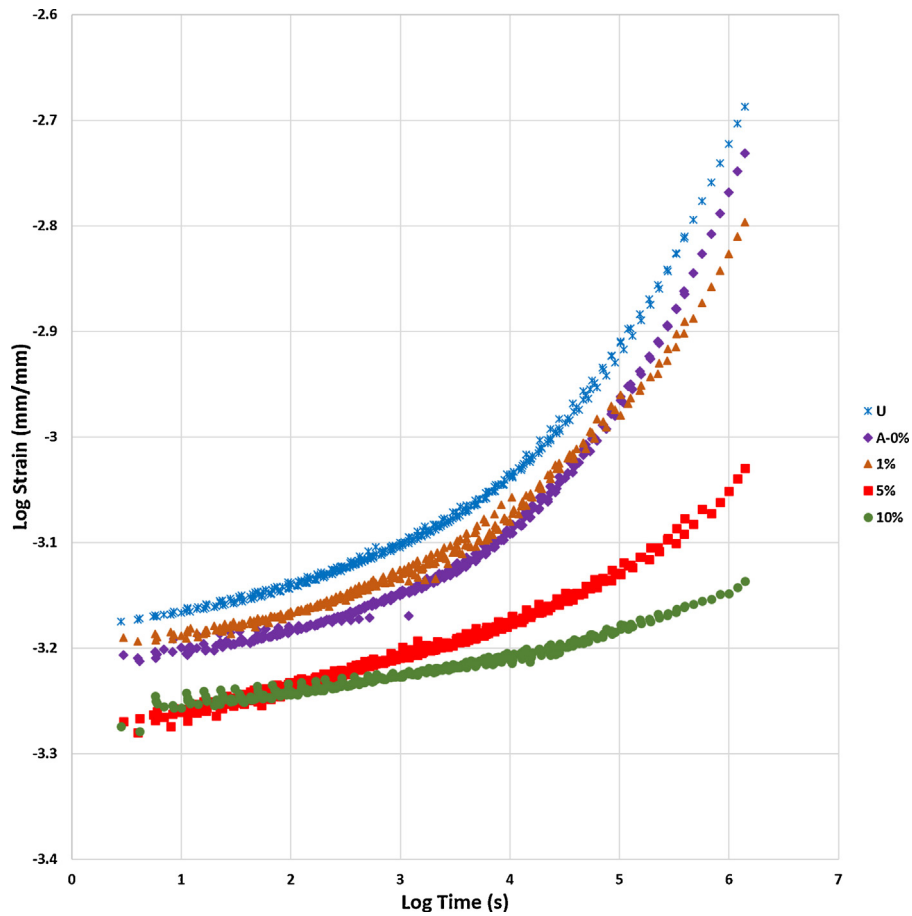

Fig. 5. TTS master curves for creep of the composites incorporated with different loadings of PJF at a reference temperature of 40 °C.

temperature (K). The master curves, which give an indication of long-term creep performance of composites, are plotted in log–log scale and presented in Fig. 5.The master curves show better creep resistance of composites with increasing content of PJF. It is obvious that the best long term performance is shown by composites incorporated with 5 and 10% PJF indicating their good reinforcing effectiveness. It is also interesting to note that above log-time 4.0 s, the creep deformation of untreated, 0 and 1% composites show a faster tendency of increase compared to 5 and 10% PJF composites. These findings show that under the small stress, the materials entered into a viscoelastic state over an extremely long period of time, and in viscoelastic state the role of 1% incorporation of PJF in the reinforcement effectiveness is less than that of 5 and 10% PJF.

Fig. 6 shows that the prediction ability of the Burger's model, Findley's model and two parameter power law model (Eqs. (2), (4) and (5)) for the log-term creep behavior of composites at the reference temperature of 40 °C. The incorporation of PJF in composites decreased the long term creep strain compared untreated and 0% filled alkali treated composites. It can be clearly seen that Findley's model is good to predict the long-term creep performance. However, this model provides the adequate prediction ability within the steady state creep and given time interval as revealed by some researchers (Siengchin, 2013; Siengchin and Karger-Kocsis, 2009) while for longer time duration the calculated data may show considerable deviation from the experimental data. The prediction of the Burger's model shows some deviation and that of two parameter power law model, shows a little large deviation from the experimental data. Similar findings were reported by other researchers (Hao et al., 2014; Jia et al., 2011). The simulated parameters of Burger, Findley and two parameters power law models are summarized in Table 2. The parameters of Burger model, resulted from fitting creep curves, are very different from those of the short term creep tests. It can be seen from Table 2 that all the Burger model parameters increase with the increase in loading of PJF%. The η_M, which determines long-term creep, is lowest for untreated composite and highest for 10% PJF composite. Therefore, the untreated composite shows the highest and 10% PJF composite shows the lowest creep deformation. It is also obvious for Findley model that the parameter a (reflecting short-term creep) increased and parameters ε_0 (reflecting the instantaneous initial creep strain) and b (reflecting log-term creep) decreased with the increasing content of PJF which indicates an enhanced long-term creep performance with PJF loading. Similarly, for two parameter power law model, parameter a (reflecting short-term creep) increased and parameter b (reflecting log-term creep) decreased with the increasing content of PJF.

3.3. Dynamic mechanical thermal properties

Dynamic mechanical thermal analysis can characterize the viscoelastic properties of the materials and determine the information of storage modulus, loss modulus (the energy dissipation associated with the motion of polymer chains) and loss factor (tan delta) of polymer composites within the measured temperature range (Wang et al., 2015). The variation of storage modulus (E') of composites incorporated with different content of PJF as a function of temperature at frequency of 1 Hz is shown in Fig. 7. It can be seen from Fig. 7a that there is a gradual fall in the storage moduli with temperature, which should be related with an energy dissipation phenomenon involving cooperative motions of the polymer chains

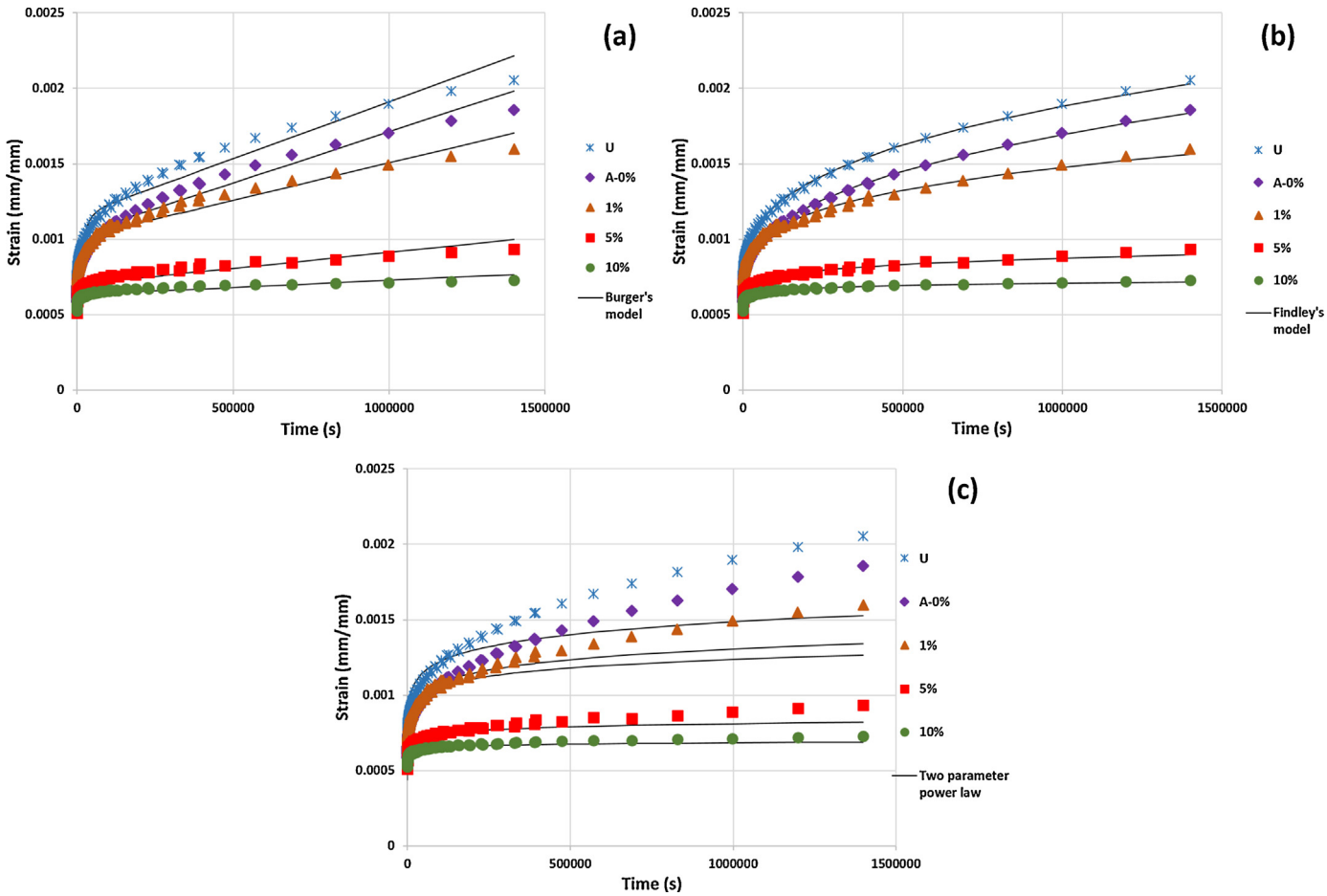

Fig. 6. Long-term creep prediction of composites by (a) Burger's model, (b) Findley model and (c) two parameter power law model at 40 °C.

Table 2
Simulated parameters of Burger's model, Findley's power law model and two parameters power law model for long term creep prediction of the composites at 40 °C.

Temperature	Parameters	Composite types				
		Untreated	Alkali-0%	1%	5%	10%
Burger's model	E_M (MPa)	2713.76 ± 193.6	3002.45 ± 184.0	2904.39 ± 179.0	3478.01 ± 191.0	3517.07 ± 125.5
	E_K (MPa)	4781.98 ± 2005.8	5470.29 ± 2194.5	6271.53 ± 2337.0	15949.06 ± 7113.4	31490.67 ± 16174.2
	η_M (Pa s)	2.64E9 ± 1.29E9	2.94E9 ± 1.29E9	4.01E9 ± 2.19E9	9.44E9 ± 6.93E9	2.10E10 ± 2.04E10
	η_K (Pa s)	1.0227E8 ± 8.73E7	1.35E8 ± 1.05E8	9.24E7 ± 7.83E7	6.76E7 ± 9.00E7	9.49E7 ± 1.53E8
	SS*	4.86566E-7	3.00571E-7	2.96188E-7	1.2249E-7	4.56987E-8
	Adj. R^2	0.9696	0.97551	0.9658	0.92279	0.88442
Findley's model	a	1.05E-5 ± 4.83E-06	6.49E-6 ± 3.69E-06	1.79E-5 ± 1.14E-05	3.49E-5 ± 3.45E-05	3.35E-5 ± 5.92E-04
	b	0.34341 ± 3.39E-02	0.3699 ± 4.22E-02	0.28033 ± 4.63E-02	0.17143 ± 6.61E-02	0.1284 ± 2.27E + 00
	ε_0	6.70E-4 ± 2.68E-05	6.17E-4 ± 2.58E-05	6.13E-4 ± 3.82E-05	5.00E-4 ± 5.74E-05	5.11E-4 ± 9.03E-03
	SS*	3.83097E-8	4.27255E-8	4.37949E-8	1.91548E-8	1.30874E-8
	Adj. R^2	0.99761	0.99653	0.99496	0.98797	0.96701
Two parameter power law model	a	4.63E-4 ± 1.41E-04	4.24E-4 ± 1.39E-04	4.82E-4 ± 1.00E-04	4.85E-4 ± 3.61E-05	5.22E-4 ± 2.08E-05
	b	0.08443 ± 3.37E-02	0.08145 ± 3.64E-02	0.06828 ± 2.37E-02	0.03723 ± 9.03E-03	0.01951 ± 5.01E-03
	SS*	2.4937E-6	2.31209E-6	1.0253E-6	9.22041E-8	2.50976E-8
	Adj. R^2	0.8452	0.8128	0.88238	0.94226	0.93694

SS*: sum of squared deviations.

with temperature (Feng et al., 2011). The increase in storage modulus over the whole temperature range was observed for composites incorporated with different loadings of PJF, for example, addition of 1, 5 and 10% PJF causes a significant increase of ~18%, 22% and 43% in the storage modulus respectively at 35 °C. Moreover, the storage modulus curves of composites have been shifted to higher temperatures after addition of the PJF, particularly 5 and 10% loading. This significant improvement in storage modulus is due to better reinforcing effect of PJF leading to increased stiffness and the mobility restriction of polymer chains (Jia et al., 2011). The change in loss factor (tan δ, the ratio of loss modulus to corresponding storage modulus) of composites with different loading of PJF as a function of temperature is shown in Fig. 7c. Untreated composite displayed a higher tan δ peak value than others. This may be attributed to more energy dissipation due to frictional damping at the weaker untreated fiber/matrix interface. The temperature at which tanδ attains a maximum value can be referred to as the glass transition temperature (T_g) (Shanmugam and Thiruchitrambalam, 2013). A positive shift in T_g can be observed for all composites incorporated with PJF compared to untreated composite The lower tanδ peak

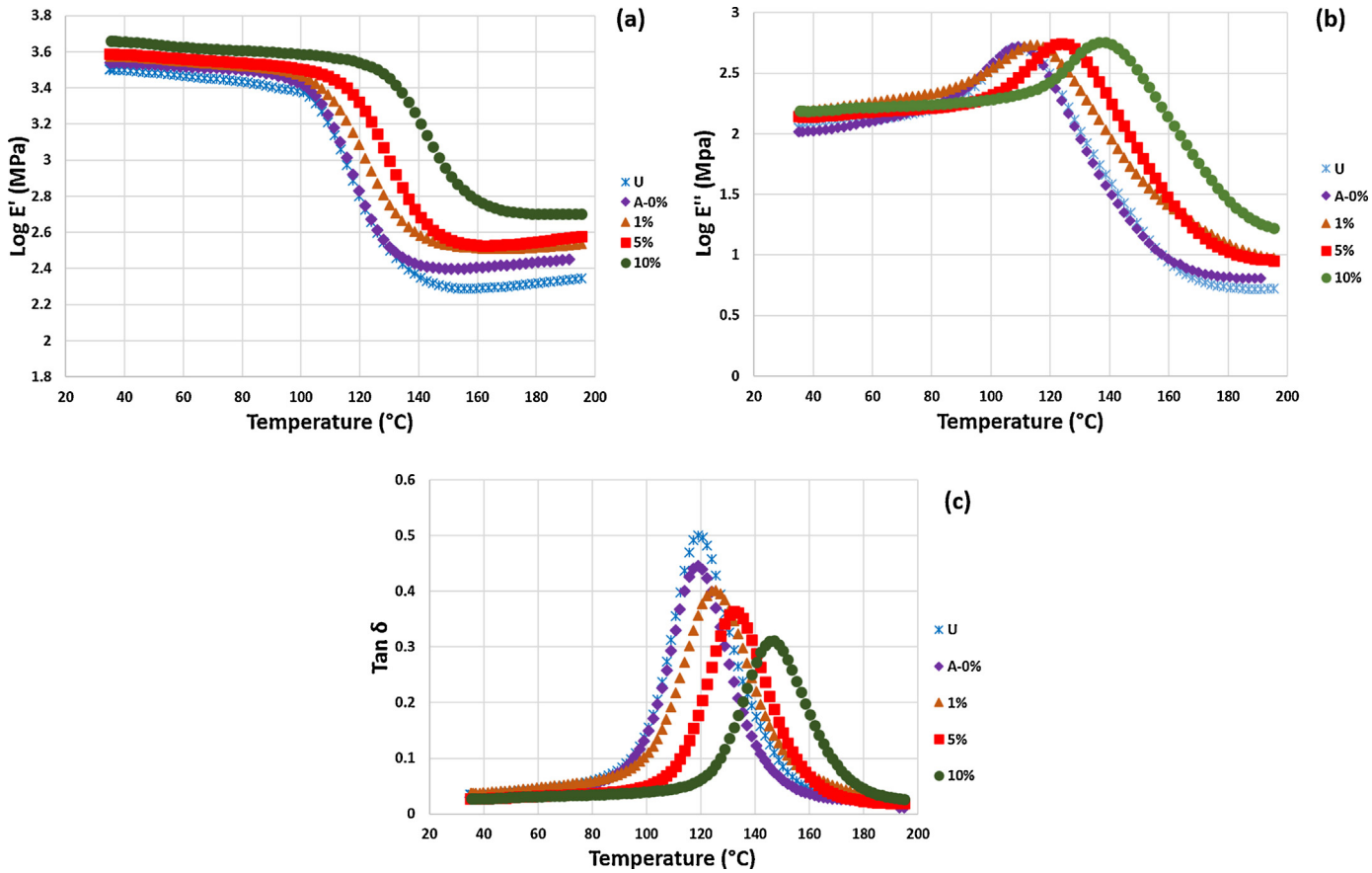

Fig. 7. Dynamic mechanical properties composites incorporated with different loadings of PJF; (a) storage modulus, (b) loss modulus, (c) tan delta.

Table 3
T_g values obtained from E'' curves.

Composites	T_g from E''_{max} curve (°C)
Untreated	110.10
Alkali-0%	110.60
1%	114
5%	123
10%	137

height is shown by composite incorporated with 10% PJF followed by 5% and 1% PJF composites, exhibiting a strong fiber/matrix interfacial interactions which can restrict the segmental movement of the polymer chains leading to the increased T_g.

It has been reported that T_g values obtained from loss modulus (E'') curve peak are more realistic as compared to those obtained from loss factor (tan δ) (Akay, 1993). A positive shift in T_g to higher temperature for all composites incorporated with PJF is observed, i.e. T_g increased from 110.1 °C for untreated to ~110.6, 114, 123 and 137 °C for composites incorporated with 0, 1, 5 and 10% PJF respectively as presented in Table 3 and Fig. 7b. This may be due to reduced mobility of matrix polymer chains and better reinforcement effect of PJF. It has been reported that systems containing more restrictions and a higher degree of reinforcement tend to exhibit higher T_g (Almeida et al., 2012).

4. Conclusion

Creep behavior of alkali treated woven jute/green epoxy composites incorporated with different loadings of chemically treated pulverized jute fibers (PJF) was presented at various environment temperatures. The creep deformation was found to increase with temperature. The creep resistance of composites was found to improve significantly with the incorporation of PJF. The modeling of creep data was satisfactorily conducted by using Burger's model, Findley's power law model and a simpler two-parameter power law model. The Burger's model fitted well the short-term creep data. However, the Findley's power law model was satisfactory for predicting the long-term creep performance of composites compared to Burger and two parameter model. The master curves, generated by TTS principle, indicated the prediction of the long-term performance of composites. Dynamic mechanical test results revealed the increase in storage modulus, glass transition temperature and reduction in the tangent delta peak height of PJF incorporated composites. Based on the analysis of results, the improved creep resistance of the composites were likely attributed to the inhibited mobility of polymer matrix molecular chains initiated by large interfacial contact area of PJF as well as their interfacial interaction with the polymer matrix.

Acknowledgements

This work was supported under the student grant scheme (SGS-21085) by Technical University of Liberec, Czech Republic. One of the authors is thankful to Dr. Ing. Antonín Potěšil and Ing. Petr Hornik for providing DMA testing facilities.

References

Acha, B.A., Reboredo, M.M., Marcovich, N.E., 2007. Creep and dynamic mechanical behavior of PP–jute composites: Effect of the interfacial adhesion. Compos. Part A Appl. Sci. Manuf. 38, 1507–1516.
Akay, M., 1993. Aspects of dynamic mechanical analysis in polymeric composites. Compos. Sci. Technol. 47, 419–423.

Almeida Jr., J.H.S., Ornaghi Jr., H.L., Amico, S.C., Amado, F.D.R., 2012. Study of hybrid intralaminate curaua/glass composites. Mater. Des. 42, 111–117.
Baheti, V., Militky, J., 2013. Reinforcement of wet milled jute nano/micro particles in polyvinyl alcohol films. Fibers Polym. 14, 133–137.
Bledzki, A.K., Faruk, O., 2004. Creep and impact properties of wood fibre–polypropylene composites: influence of temperature and moisture content. Compos. Sci. Technol. 64, 693–700.
Cai, Y., David, S., Pailthorpe, M., 2000. Dyeing of jute and jute/cotton blend fabrics with 2: 1 pre-metallised dyes. Dye Pigm. 45, 161–168.
Feng, Q.-P., Shen, X.-J., Yang, J.-P., Fu, S.-Y., Mai, Y.-W., Friedrich, K., 2011. Synthesis of epoxy composites with high carbon nanotube loading and effects of tubular and wavy morphology on composite strength and modulus. Polymers 52, 6037–6045.
Findley, W.N., Davis, F.A., Onaran, K., 1989. Creep and Relaxation of Nonlinear Viscoelastic Materials: With an Introduction to Linear Viscoelasticity. Dover Publications, Inc., New York.
Hao, A., Chen, Y., Chen, J.Y., 2014. Creep and recovery behavior of kenaf/polypropylene nonwoven composites. J. Appl. Polym. Sci. 131.
Haque, M.M., Hasan, M., Islam, M.S., Ali, M.E., 2009. Physico-mechanical properties of chemically treated palm and coir fiber reinforced polypropylene composites. Biores. Technol. 100, 4903–4906.
Jia, Y., Peng, K., Gong, X.-l., Zhang, Z., 2011. Creep and recovery of polypropylene/carbon nanotube composites. Int. J. Plast. 27, 1239–1251.
John, M.J., Anandjiwala, R.D., 2009. Chemical modification of flax reinforced polypropylene composites. Compos. Part A Appl. Sci. Manuf. 40, 442–448.
Krempl, E., Khan, F., 2003. Rate (time)-dependent deformation behavior: an overview of some properties of metals and solid polymers. Int. J. Plast. 19, 1069–1095.
Liu, W., Mohanty, A., Drzal, L., Askel, P., Misra, M., 2004. Effects of alkali treatment on the structure, morphology and thermal properties of native grass fibers as reinforcements for polymer matrix composites. J. Mater. Sci. 39, 1051–1054.
Marcovich, N.E., Villar, M.A., 2003. Thermal and mechanical characterization of linear low-density polyethylene/wood flour composites. J. Appl. Polym. Sci. 90, 2775–2784.
Meloun, M., Militky, J., 2011. Statistical Data Analysis: A Practical Guide. Woodhead Publishing, Limited.
Militký, J., Jabbar, A., 2015. Comparative evaluation of fiber treatments on the creep behavior of jute/green epoxy composites. Compos. Part B Eng. 80, 361–368.
Mishra, S., Mohanty, A.K., Drzal, L., Misra, M., Parija, S., Nayak, S.K., Tripathy, S.S., 2003. Studies on mechanical performance of biofibre/glass reinforced polyester hybrid composites. Compos. Sci. Technol. 63, 1377–1385.
Mishra, R., Baheti, V., Behera, B., Militky, J., 2014. Novelties of 3-D woven composites and nanocomposites. J. Text. Inst. 105, 84–92.
Morshed, M., Alam, M., Daniels, S., 2010. Plasma treatment of natural jute fibre by RIE 80 plus plasma tool. Plas. Sci. Technol. 12, 325.
Plaseied, A., Fatemi, A., 2008. Tensile creep and deformation modeling of vinyl ester polymer and its nanocomposite. J. Reinf. Plast. Compos. 28, 1775–1788.
Shanmugam, D., Thiruchitrambalam, M., 2013. Static and dynamic mechanical properties of alkali treated unidirectional continuous palmyra palm leaf stalk fiber/jute fiber reinforced hybrid polyester composites. Mater. Des. 50, 533–542.
Shen, L., Phang, I.Y., Chen, L., Liu, T., Zeng, K., 2004. Nanoindentation and morphological studies on nylon 66 nanocomposites. I. Effect of clay loading. Polymers 45, 3341–3349.
Siengchin, S., 2013. Dynamic mechanic and creep behaviors of polyoxymethylene/boehmite alumina nanocomposites produced by water-mediated compounding Effect of particle size. J. Thermo. Compos. Mater. 26, 863–877.
Siengchin, S., Karger-Kocsis, J., 2009. Structure and creep response of toughened and nanoreinforced polyamides produced via the latex route: effect of nanofiller type. Compos. Sci. Technol. 69, 677–683.
Tajvidi, M., Falk, R.H., Hermanson, J.C., 2005. Time–temperature superposition principle applied to a kenaf-fiber/high-density polyethylene composite. J. Appl. Polm. Sci. 97, 1995–2004.
Tserki, V., Zafeiropoulos, N., Simon, F., Panayiotou, C., 2005. A study of the effect of acetylation and propionylation surface treatments on natural fibres. Compos. Part A Appl. Sci. Manuf. 36, 1110–1118.
Wang, X., Gong, L.-X., Tang, L.-C., Peng, K., Pei, Y.-B., Zhao, L., Wu, L.-B., Jiang, J.-X., 2015. Temperature dependence of creep and recovery behaviors of polymer composites filled with chemically reduced graphene oxide. Compos. Part A Appl. Sci. Manuf. 69, 288–298.
Ward, I.M., Sweeney, J., 2012. Mechanical Properties of Solid Polymers. John Wiley & Sons.
Xu, Y., Wu, Q., Lei, Y., Yao, F., 2010. Creep behavior of bagasse fiber reinforced polymer composites. Biores. Technol. 101, 3280–3286.
Yang, J.-L., Zhang, Z., Schlarb, A.K., Friedrich, K., 2006a. On the characterization of tensile creep resistance of polyamide 66 nanocomposites. Part I. Experimental results and general discussions. Polymers 47, 2791–2801.
Yang, J.-L., Zhang, Z., Schlarb, A.K., Friedrich, K., 2006b. On the characterization of tensile creep resistance of polyamide 66 nanocomposites. Part II: modeling and prediction of long-term performance. Polymers 47, 6745–6758.